Effect of dielectric barrier on rectification, injection and transport properties of printed organic diodes

K E Lilja, H S Majumdar, K Lahtonen, P Heljo, S Tuukkanen, T Joutsenoja, M Valden, R Österbacka, D Lupo

To cite this version:

K E Lilja, H S Majumdar, K Lahtonen, P Heljo, S Tuukkanen, et al.. Effect of dielectric barrier on rectification, injection and transport properties of printed organic diodes. Journal of Physics D: Applied Physics, IOP Publishing, 2011, 44 (29), pp.295301. 10.1088/0022-3727/44/29/295301 . hal-00636198

HAL Id: hal-00636198
https://hal.archives-ouvertes.fr/hal-00636198

Submitted on 27 Oct 2011

HAL is a multi-disciplinary open access archive for the deposit and dissemination of scientific research documents, whether they are published or not. The documents may come from teaching and research institutions in France or abroad, or from public or private research centers.

L'archive ouverte pluridisciplinaire **HAL**, est destinée au dépôt et à la diffusion de documents scientifiques de niveau recherche, publiés ou non, émanant des établissements d'enseignement et de recherche français ou étrangers, des laboratoires publics ou privés.

Effect of dielectric barrier on rectification, injection and transport properties of printed organic diodes.

K E Lilja[1,4], H S Majumdar[2], K Lahtonen[3], P Heljo[1], S Tuukkanen[1], T Joutsenoja[1], M Valden[3], R Österbacka[2] and D Lupo[1]

[1]Tampere University of Technology, Department of Electronics, P.O. Box 692, FI-33101 Tampere, Finland

[2]Åbo Akademi University, Department of Natural Science and Center for Functional Materials, Porthansgatan 3, FI-20500, Turku, Finland

[3]Tampere University of Technology, Surface Science Laboratory, P.O. Box 692, FI-33101 Tampere, Finland

E-mail: kaisa.lilja@tut.fi

[4]Author to whom any correspondence should be addressed.

Abstract. Rectification ratios of 10^5 were observed in printed organic copper/polytriarylamine (PTAA)/silver diodes with a thin insulating barrier layer at the copper/PTAA interface. To clarify the origin of the high rectification ratio in the diodes, the injection, transport and structure of the diodes with two different copper cathodes were examined using impedance spectroscopy and X-ray photoelectron spectroscopy (XPS). The impedance data confirm that the difference in diode performance arises from the copper/PTAA interface. The XPS measurements show that the copper surface in both diode structures is covered by a layer of Cu_2O topped by an organic layer. The organic layer is thicker on one of the surfaces, which results in lower reverse currents and higher rectification ratios in the printed diodes. We suggest a model where a dipole at the dual insulating layer induces a shift in the semiconductor energy levels explaining the difference between the diodes with different cathodes.

1. Introduction

The foreseen advantages of organic semiconductor materials rely on the possibility to fabricate electronic components and circuits using cost-effective manufacturing processes. This requires solution processable materials and fundamental research on organic electronic components, such as

diodes and transistors. Previously, high-throughput gravure printing processes have been demonstrated for organic light emitting diodes and transistors [1-4]. Also, gravure printed organic Schottky diodes have been demonstrated as RFID rectifiers and as the active components in display driving circuitry [5, 6]. In these applications, the organic diode needs to exhibit a sufficient rectification ratio and forward current.

Recently we showed that processing and device architecture have a significant effect on the performance of printed organic diodes with one or more Schottky contacts [7]. The diodes exhibited very low currents under reverse bias despite the low Schottky barrier. Furthermore, a thin interfacial barrier layer was found to prevent hole injection from the cathode electrode into the organic semiconductor under reverse bias without having a significant effect on the forward bias current, leading to a higher rectification ratio. It is unlikely that the observed Schottky barrier of 0.1 to 0.3 eV, albeit combined with a tunnelling barrier, could completely explain rectification ratios of 10^3 to 10^5. In this article we clarify the origin of the high rectification in the diodes and their improvement upon adding an additional dielectric layer.

The interfacial phenomena at metal/organic interfaces have been described in detail both from theoretical and modelling perspectives [8, 9]. One of the most important effects in determining the electrical structure of the contact is Fermi-level pinning of the semiconductor. Here, we verify the different behaviour of two diode structures by using impedance spectroscopy, which has been used by several groups to study the behaviour of metal/organic interfaces and interfacial layers in organic (light-emitting) diode structures [10-14]. X-ray photoelectron spectroscopy (XPS) is a well-known characterization method for determining the chemical composition and depth distribution of elements on the surface of various materials. We use XPS to find detailed information of the diode cathode interface by examining the Cu LMM transitions and the in-depth chemical composition of the copper electrodes. Based on these results, the previously presented model for charge carrier movement across the barrier layer at the cathode interface is extended and the origin of the high rectification ratio in these diodes discussed.

2. Materials and methods

The diodes were fabricated using roll-to-roll compatible printing processes. A copper cathode layer was deposited either by vacuum evaporation or sputtering onto a poly(ethylene terephthalate) (PET) film and patterned by shadow masking or wet etching. The polytriarylamine (PTAA) semiconductor layer, and anode (silver) inks were printed with a laboratory-scale gravure printing press (Labratester Automatic from Norbert Schläfli Maschinen) and cured at 115 ºC. The diodes were fabricated in a dust-free environment (close to ISO 14644-1 class 5) at room temperature.

The DC current density - voltage (*J*-*V*) -characteristics of the diodes were measured using a Keithley 236 Source-Measure Unit under ambient laboratory conditions. The diode capacitances were measured using a HP 8752A Network Analyzer at a frequency of 10 MHz and 22 mV rms. Impedance spectroscopy was done with a Gamry 600™ Potentiostat in a frequency range of 10 Hz to 1 MHz. The amplitude of the AC bias was 20 mV rms. The DC bias was varied from 0.1 V to 5.0 V.

The chemical composition and thicknesses of the surface layers on the copper cathodes were analyzed utilizing nonmonochromatized dual anode X-ray photoelectron spectrometer (ESCA3000 XPS, VG Microtech Inc., UK) located in an ultra-high vacuum (UHV) system with a base pressure of $<1\times10^{-10}$ mbar. The UHV system is described in detail elsewhere [15]. The XPS measurements were performed ex situ on substrates that had been stored under ambient laboratory conditions prior to measurement. 0° emission angle and both, Al Kα and Mg Kα radiations were utilized for excitation. For the measurements, ~8×8 mm^2 pieces of PET substrates with Cu cathodes were cut from larger sheets. The elemental concentrations on both Cu surfaces were determined from a circular detection area of ~600 μm in diameter on four different non-overlapping positions. The XPS high-resolution spectra of C 1s, O 1s, Cu 2p and Cu LMM peaks were analysed. The analysis procedure of the Cu LMM transition is described elsewhere in more detail [16]. The inelastic electron energy-loss background thickness analysis was performed with QUASES software package [17], using reference spectra of experimentally obtained line shapes of metallic Cu, Cu_2O and PET. The error of the inelastic electron energy-loss background analysis method is ±10% in coverage and ±20% in thickness.

The surface topography of the copper cathodes was characterized by AFM using Veeco Dimension 3001 with silicon cantilevers in tapping mode. Image analysis was performed using Nanoscope 6.13R1 software. The AFM measurements were done under ambient laboratory conditions.

3. Results and Discussion

The log *J*- log *V* -characteristics of the diodes with evaporation-deposited [Cu(e)] and sputter-deposited [Cu(s)] copper cathodes are presented in figure 1. The diodes are under forward bias when the silver electrode is biased positively with respect to the copper electrode. For Cu(e) diodes the current turned to space-charge limited at around an applied voltage of 0.2 V. For Cu(s) diodes the current was injection limited up to about 2 V, above which the current approached space-charge limited behaviour. Furthermore, the rectification ratio improved from 10^3 to 10^5 due to the lower reverse current of the Cu(s) diodes. The Schottky barriers, 0.3 eV and 0.1 eV for Cu(e) and Cu(s), respectively [7], do not explain the difference in the current levels. Therefore, we argue that an additional interfacial effect is responsible for the observed high rectification ratio in the Cu(s) diodes.

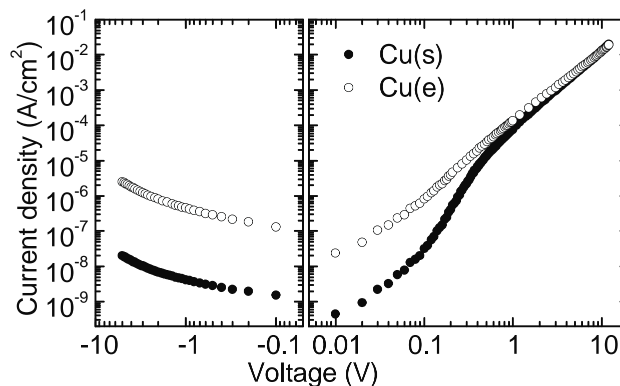

Figure 1. Log *J*- log *V* -performance of diodes with sputter-deposited [Cu(s)] and evaporation-deposited [Cu(e)] copper cathodes.

Impedance spectroscopy was used to demonstrate that the difference in diode characteristics is due to the metal/semiconductor interface. Measurements were done on Cu(e) and Cu(s) diodes in a frequency range of 10 Hz to 1 MHz. Additionally, the diode capacitances were measured at 10 MHz using the HP 8752A Network Analyzer. At MHz frequencies only the bulk capacitance of the semiconductor was observed. It was found that the bulk capacitances were the same for both diodes. However, the impedance data revealed differences that concurred with the *J*-*V* -characteristics. Figure 2 shows the Cole-Cole plots of the complex impedance (*Z*) measured in the Cu(e) (open circle) and Cu(s) (closed circle) diodes. The frequency in the plots increases from right to left. For a DC bias of 5.0 V there was no difference between the impedance of the diodes [figure 2(a)], but as the DC bias was decreased a distinct difference was observed. As seen also in the *J*-*V* -data, a difference between the diodes started to appear at voltages below ~0.5 V. In the impedance data, the difference systematically increased for dc biases of 0.4 V [figure 2(b)], 0.2 V [figure 2(c)] and 0.1 V [figure 2(d)]. The important observation from the impedance data and from the capacitance measurement is that though the bulk capacitance of the semiconductor layer in the diode did not change, the overall impedance of the diodes varied as a function of the applied bias voltage. Since the only difference between the diodes is the copper/semiconductor interface, it is safe to conclude that the impedance difference between the diodes is from the variation of the cathode interface. The fact that the difference is most pronounced in the low frequency region also corroborates with the fact that the variation is an interfacial effect.

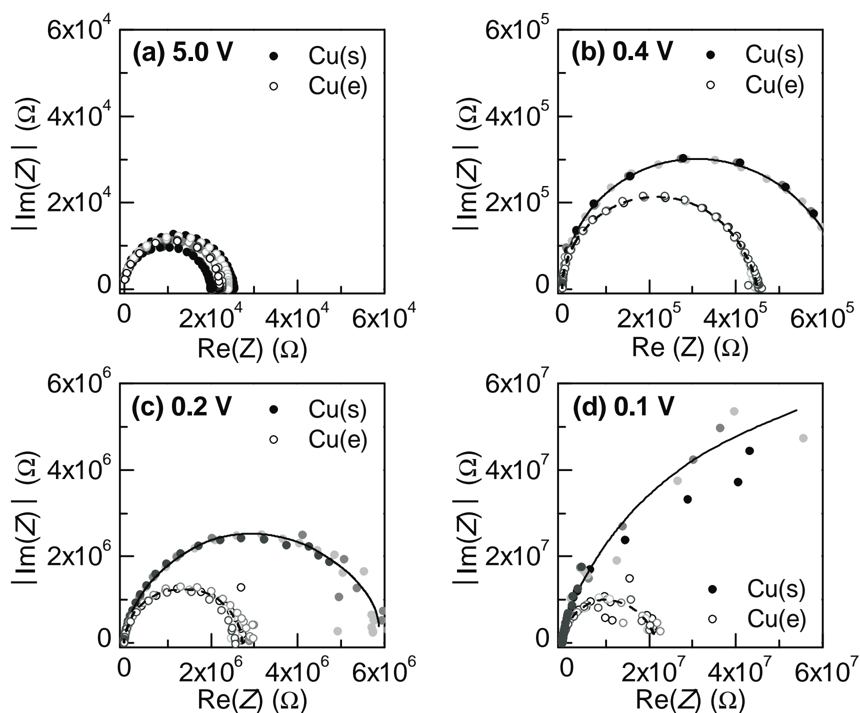

Figure 2. Cole-Cole plots of the diode impedance with sputter-deposited [Cu(s), closed circle] and evaporation-deposited [Cu(e), open circle] copper cathodes at forward bias voltages of 5.0 V, 0.4 V, 0.2 V and 0.1 V. The frequency increases from right to left from 10 Hz to 1 MHz.

Efforts were made to fit the experimental impedance data to formulate an equivalent circuit for the diode structures. It was possible to reasonably fit the data for 5.0 V DC bias with one parallel RC circuit that represented only the PTAA bulk. Whereas the real capacitance value obtained for the bulk agreed with the capacitance value obtained from the high frequency measurements, it was not possible to find a suitable equivalent circuit for the diodes at low DC bias. This is most likely due to the pronounced role of the interfaces on injection and transport at low biases as well as parasitic capacitances from measurement wires and printed conductor lines. Also, the conductivity and dielectric constant of the semiconductor can be frequency dependent which complicates the RC fitting using simple RC elements [11].

Previously we observed indications of an organic layer covering the surface of the Cu(s) substrate [7]. This analysis was based on the survey spectrum, C 1s and O 1s peaks of the XPS signal intensity with binding energies from 0 to 1100 eV. Here we report the results based on a more detailed XPS study, including analysis of the surface in-depth chemical structure and copper oxidation state. Figure 3 represents the Al Kα -excited survey spectra and Cu LMM transitions of the Cu(e) and Cu(s) surfaces. As shown in figure 3(a), the Cu(s) surface contained a higher relative concentration of carbon and attenuated copper signals. The results were comparable to earlier results and suggested

that the Cu(s) surface is covered by an organic layer. Carbon was also detected on the Cu(e) surface where the copper signals are stronger indicating carbon impurities on top of the surface.

The X-ray excited Auger peaks of copper at 568.3, 568.8 and 570.0 eV can be assigned to metallic Cu, Cu (II) and Cu (I) -oxidation states, respectively. The $L_3M_{45}M_{45}$ transitions of the Cu(e) and Cu(s) surfaces are shown in figure 3(b). The shapes of the Cu LMM transition and shake-up satellites of the Cu 2p (not shown) indicated that the copper was mostly as Cu (I), presumably as Cu_2O, since the substrates were stored in ambient air after fabrication. Low amounts of higher Cu oxidation states (max. ~15% of Cu) may also exist in the interfacial layer. The sampling depth of the Cu LMM signal through the Cu_2O and organic layer is in the order of 6–7 nm. On both surfaces the metallic Cu LMM signal was observed. Thus, if uniform layer thicknesses are assumed, the metallic Cu layer is buried less than 7 nm deep below the other layers.

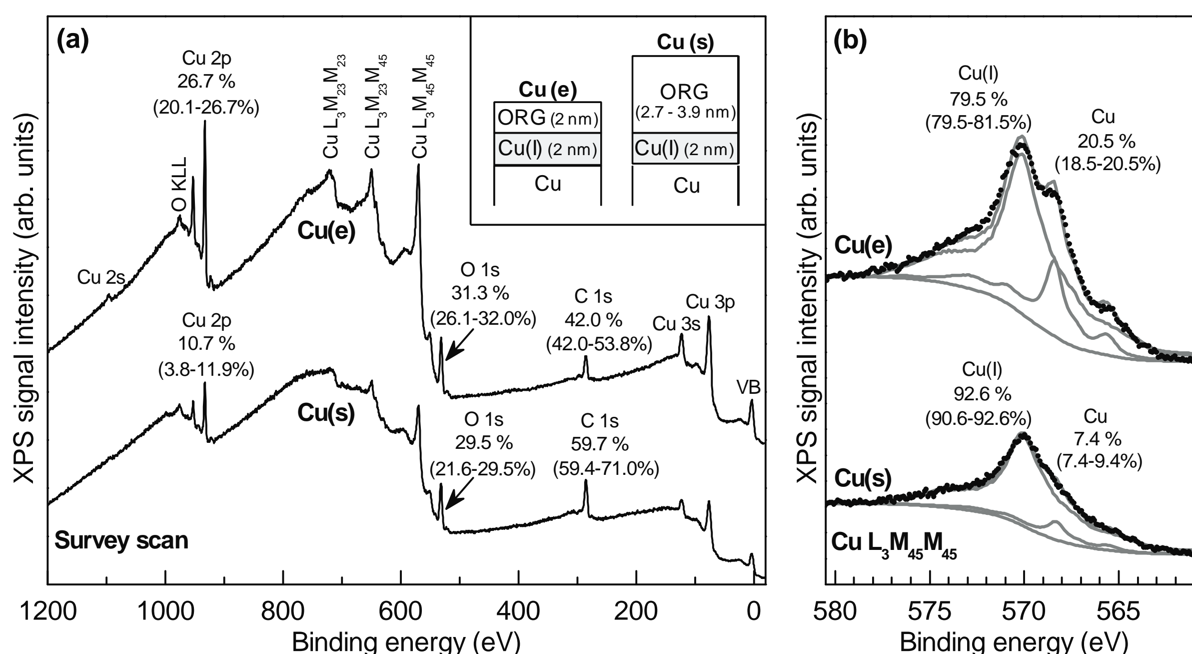

Figure 3. (a) Survey spectra and (b) Cu $L_3M_{45}M_{45}$ transitions of the evaporation-deposited [Cu(e)] and sputter-deposited [Cu(s)] surfaces. The atomic concentrations of Cu, O, and C are indicated in the figure. The upper values are for the shown spectra. The values in brackets indicate the variation range of four different non-overlapping positions on the samples. The inset shows a schematical presentation of the surface layers, where ORG is the organic layer and Cu(I) is the Cu_2O layer on top of the metallic copper.

Previously we speculated that the organic layer would be PET coming from the substrate in the sputter-deposition process [7]. However, the recent XPS results show that the C-C/C-O and C-C/C=O ratios in the organic layer on Cu(s) and Cu(e) are higher than on a PET reference. This may indicate

that the surfaces contain other hydrocarbon impurities besides pure PET, i.e. the C-C component originates partly from the aromatic ring in PET, and partly from other hydrocarbons. In addition, since all chemical compounds that contain C-C bonds induce XPS peak(s) near 285 eV in binding energy, we cannot be affirmative that the layer is PET.

More accurate layer thicknesses on the copper surfaces were calculated based on the analysis of the inelastic electron energy-loss backgrounds and main peaks of the Mg Kα -excited Cu 2p and C KVV transitions. According to the in-depth chemical analysis, the thickness of the organic layer (ORG) on Cu(s) varied between 2.7 and 3.9 nm, and the thickness of the Cu_2O layer was 2 nm, as presented in the inset of figure 3. Using the same reference spectra for Cu(e), the thickness of the organic layer was 2 nm and Cu_2O layer 2 nm. The exploited buried layer morphology model is simplified, and quality of the fitting was lower with Cu(e), indicating that the actual layer thickness is not absolutely uniform and the layer may have pinholes or island formation. AFM experiments showed that the surface roughness R_a of both Cu(s) and Cu(e) was 2-4 nm.

Based on the *J-V* -characteristics, only the Ag electrode had ohmic contact with PTAA whereas the Cu contact created an injection barrier for both, Cu(e) and Cu(s). Since the measured work functions of Cu, printed Ag and the HOMO of PTAA are quite similar (4.8 – 5.2 eV) [7], charge carriers should be injected from both the electrodes under proper bias conditions. If there would be pinholes or islands in the interfacial layer, that would lead to leakage current due to injection from Cu in the order similar to what was observed for injection from Ag. Since this is not the case, and the AFM data does not reveal the existence of islands, we conclude that the interfacial layer on top of the Cu is uniform.

We argue that the difference between the diodes is due to the observed interfacial layer on the cathode contact. In fact, *both* the organic layer and the Cu_2O layer are likely to have an effect on the charge carrier movement across the cathode/semiconductor interface. The prior hypothesis for the diode function in reverse bias was that since the semiconductor is fully depleted and there are no charge carriers that could create a sufficient field across the interfacial barrier to assist tunnelling through the barrier, the reverse current in the Cu(s) diodes is very low. [7] Based on the XPS and impedance data the hypothesis can be extended using the dual (Cu_2O + organic) insulating layer, as presented in figure 4. Since the measured Schottky barrier Φ_B, determined as the difference between the metal work function Φ_M and the HOMO of the semiconductor, is as low as 0.1 - 0.3 eV, as presented in figure 4(a), it is probable that an additional contact effect induces a higher Schottky barrier once the copper and the semiconductor are brought into contact [figures 4 (b-e)]. This can be understood in terms of (de)pinning of the semiconductor Fermi-level and dipole formation between the two dielectric materials, which have been extensively explained both for organic and inorganic semiconductor materials and are caused either by wave functions of electrons in the metal that tail into the

semiconductor or by bond polarization [8, 9, 18-21]. In practice this means that close contact between a metal and a semiconductor will cause the semiconductor energy levels to pin at a certain level. An insulator between the materials will cause a change in the pinning [19]. If there are two dielectric materials instead of one, the pinning is also affected by the orientation of the dipole potential between the two dielectrics [20]. The origin of this dipole potential is not very clear and it has been suggested to arise from Maxwell-Wagner instability of two dielectrics with different conductances [21]. Nevertheless, the presence and the effect of the dual-dielectric layer in our diodes are unquestionable. In the case of the Cu(e) diodes, we know from the XPS data that there is a dual barrier of Cu_2O and an organic layer. This causes a shift in the pinning level and, eventually, an increase in the Schottky barrier, as illustrated in figure 4(b). An increase in the Schottky barrier means that only a few charge carriers flow from the copper to the semiconductor under reverse bias and the reverse current is low, which results in a rectification ratio of 10^3.

Furthermore, the XPS data showed that there is a dual layer of Cu_2O and a thicker layer of organic material on the Cu(s) surface. This thicker dielectric layer enhances the effect of the dipole layer, as has been seen before for inorganic diodes [19]. A further increase in the Schottky barrier is observed, as depicted in figure 4(c). Due to the higher Schottky barrier, even fewer charge carriers are able to flow from the copper to the semiconductor under reverse bias and the reverse current is further lowered, leading to a higher rectification ratio of 10^5. However, as argued in the previous work [7], in forward bias the field is still high enough to assist tunnelling through the barrier, as illustrated in figure 4(d) and (e). This leads to identical diode behaviour in Cu(s) and Cu(e) diodes at a sufficiently high forward bias.

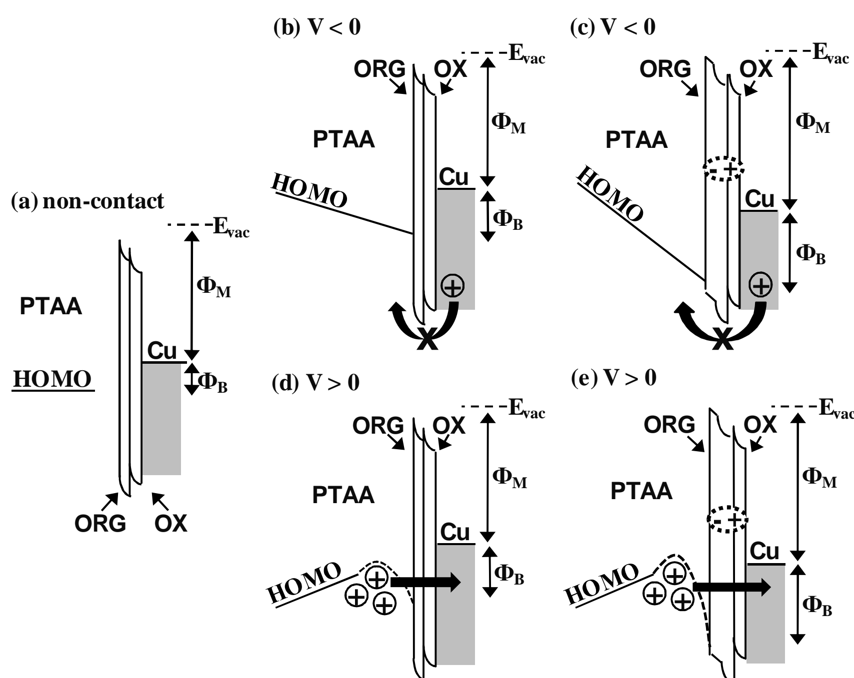

Figure 4. Simplified model for the diode Schottky contact. E_{vac} is the vacuum energy level. Φ_M is the metal work function in vacuum and Φ_B is the potential (Schottky) barrier. OX represents the Cu(I)-oxide and ORG represents the organic layer on top of the copper surface.

4. Conclusions

The effect of an insulating barrier on the rectification ratio, injection and transport properties of printed organic Schottky diodes was examined. Impedance spectroscopy showed the variation in interfacial behaviour of the two different diode structures. The XPS results further showed that an insulating layer consisting of Cu_2O and organic material exists on the Cu electrode. A 2 orders of magnitude better rectification ratio was observed for the diodes with a thicker dielectric layer. We discussed these results in light of Fermi level pinning at the copper/semiconductor interface in the presence of a thin dual dielectric layer with an intrinsic dipole potential. This explains the origin of high rectification in diodes made from metals with almost similar work-functions and, even further, the variation of the rectification with a change in the dielectric thickness. The proposed method is a successful recipe for fabricating printed, organic thin-film diodes for printed electronics applications.

Acknowledgments

The authors acknowledge UPM-Kymmene Corporation for financial support and Merck Chemicals Ltd. for providing the semiconductor material. H S Majumdar also acknowledges partial financial support from the Academy of Finland (project number 280007281) through the Center of Excellence program.

References

[1] Kopola P, Tuomikoski M, Suhonen R and Maaninen A 2009 *Thin Solid Films* **517** 5757-62

[2] Hambsch M, Reuter K, Stanel M, Schmidt G, Kempa H, Fügmann U, Hahn U and Hübler A C 2010 *Mat. Sci. Eng. B* **170** 93-98

[3] Chung D-Y, Huang J, Bradley D D C and Campbell A J 2010 *Org. Electron.* **11** 1088-95

[4] Vornbrock A de la F, Sung D, Kang H, Kitsomboonloha R and Subramanian V 2010 *Org. Electron.* **11** 2037-44

[5] Lilja K E, Bäcklund T G, Lupo D, Hassinen T and Joutsenoja T 2009 *Org. Electron.* **10** 1011-14

[6] Lilja K E, Bäcklund T G, Lupo D, Virtanen J, Hämäläinen E and Joutsenoja T 2010 *Thin Solid Films* **518** 4385-89

[7] Lilja K E, Majumdar H S, Pettersson F S, Österbacka R and Joutsenoja T 2011 *ACS Appl. Mater. Interfaces* **3** 7-10

[8] Ishii H, Sugiyama K, Ito E and Seki K 1999 *Adv. Mater.* **11** 605-25

[9] Braun S, Salaneck W R and Fahlman M 2009 *Adv. Mater.* **21** 1450-72

[10] Taylor D M and Gomes H L 1995 *J. Phys. D: Appl. Phys.* **28** 2554-68

[11] Meier M, Karg S and Riess W 1997 *J. Appl. Phys.* **82** 1961-66

[12] Scherbel J, Nguyen P H, Paasch G, Brütting W and Schwoerer M 1998 *J. Appl. Phys.* **83** 5045-55

[13] Drechsel J, Pfeiffer M, Zhou X, Nollau A and Leo K 2002 *Synth. Metals* **127** 201-5

[14] Kim S H, Jang J W, Lee K W, Lee C E and Kim S W 2003 *Solid State Commun.* **128** 143-6

[15] Lahtonen K, Lampimäki M, Jussila P, Hirsimäki M and Valden M 2006 *Rev. Sci. Instrum.* **77** 083901

[16] Lampimäki M, Lahtonen K, Hirsimäki M and Valden M 2007 *Surf. Interface Anal.* **39** 359-66

[17] Tougaard S 2003 *QUASES: Software for quantitative XPS/AES of surface nanostructures by analysis of the peak shape and background (Version 5.0)* (Odense, Denmark: University of Southern Denmark) http://www.quases.com

[18] Hu J, Wong H-S P and Saraswat K 2011 *MRS Bulletin* **36** 112-9

[19] Nishimura T, Kita K and Toriumi A 2008 *Applied Physics Express* **1** 051406

[20] Coss B E, Loh W-Y, Wallace R M, Kim J, Majhi P and Jammy R 2009 *Appl. Phys. Lett.* **95** 222105

[21] Jinesh K B, Lamy Y, Klootwijk J H and Besling W F A 2009 *Appl. Phys. Lett.* **95**, 122903